ACS OMEGA

Open Access

http://pubs.acs.org/journal/acsodf

Article

Preparation and Characterization of a Biobased Temporary Plugging Material: Self-Healing and Degradable

Jia Li,* Ming Wen, Shuang Liu, and Qiang Liu

Cite This: *ACS Omega* 2023, 8, 36207−36217

Read Online

ACCESS | Metrics & More | Article Recommendations

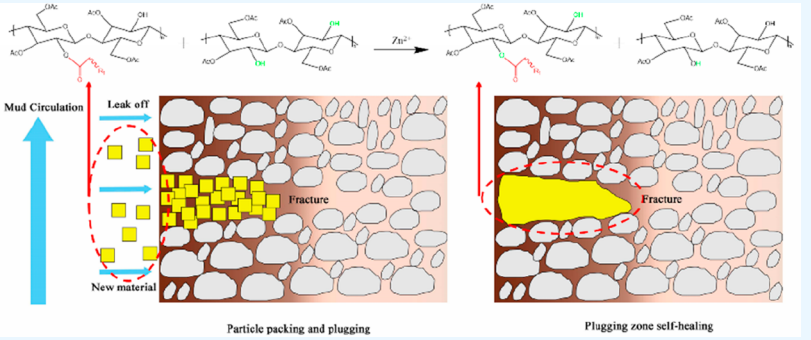

ABSTRACT: Due to the low success rate in high-temperature gas well drilling or workover operations, a new type of biobased temporary sealing material was synthesized using vanillin, succinic anhydride (SA), cellulose, and acetylacetone zinc hydrate (AZH) as catalysts. Infrared analysis proved the synthesis of vanillin-derived epoxy and the formation of a vitrimer with hydroxyl ester. The results of thermodynamic properties tests show that it has excellent thermal stability with a high glass transition temperature (T_g). The dynamic mechanical test results show that the characteristic relaxation time of the material at 120 °C is 3500 s and the self-healing rate can reach 61% within 20 min. The test results of mechanical properties show that under 10 MPa pressure, it has good elastic deformation performance, the rebound rate is more than 36%, and the crushing rate is less than 17%. The degradation performance results show that the decomposition increases to 80% under 120 °C and 1.2% NaOH. The comprehensive performance evaluation results show that the new temporary plugging material has good compatibility, and its plugging performance is better than those of a gel, composite material, and shape memory polymer. The maximum fracture plugging capacity is 5 × 4 mm, with a pressure up to 10 MPa.

1. INTRODUCTION

Natural gas resources are abundant and widely distributed and belong to clean energy. High-temperature deep shale gas and tight gas are the main development directions of oil and gas resources at present. Bedding structures or fractures are usually developed in the buried strata of these kinds of resources, and complex accidents such as lost circulation are often encountered during drilling or workover. If it cannot be handled in time, complex situations of blowout and sticking frequently happen.[1−3] The invasion of external fluid caused by lost circulation will also cause reservoir damage, increasing the cost of subsequent reservoir stimulation, reconstruction, and maintenance.

At present, studies on new high-temperature plugging materials have mainly focused on temperature-sensitive intelligent materials.[4−8] Tian et al.[9] prepared cement-based intelligent leak curing materials by using NiTi shape memory alloy through a heat treatment process. The material can block holes with a diameter of 1.5 cm at 90 °C, and its pressure-bearing capacity is greater than 12 MPa, which can better solve the problem of cavernous leakage. Mansour et al.[10−12] used the shape memory characteristics of thermosetting epoxy resin to carry out experimental research on fracture sealing. The material can adjust the activation temperature according to the demand of formation temperature, and a millimeter-scale fracture plugging experiment was carried out. Gong et al.[13] developed a self-healing hydrogel, which can realize rapid self-healing through the unique dual physical cross-linking network and the hydrogen bond between polymers. The novel material has good mechanical properties, with a tensile strength of 1230 KPa and toughness of 1250 KJ/m^3. However, the intelligent materials above are faced with the disadvantage of being

Received: June 29, 2023
Accepted: August 24, 2023
Published: September 22, 2023

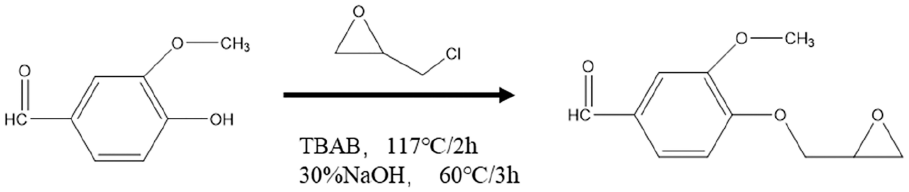

Figure 1. Synthesis route of vanillin-derived epoxy.

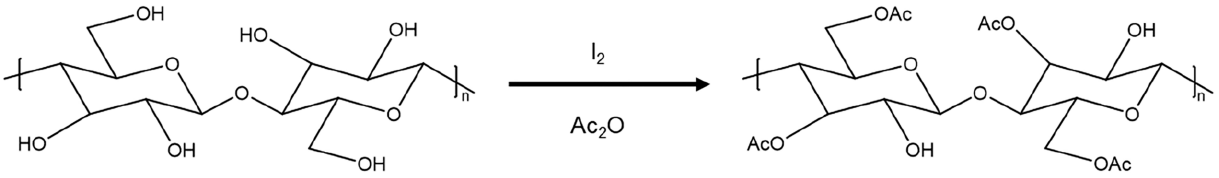

Figure 2. Modification mechanism of cellulose with partial hydroxyl substitution.

difficult to degrade. In addition, the preparation of memory alloy is more complex and the cost is higher. The temperature-sensitive expansion property of shape memory resin material is difficult to control, and the material often expands before entering the fracture. The self-healing gel is mainly used in biological and medical fields. Its temperature resistance is generally not more than 100 °C, and its strength is low. It is difficult to form an effective sealing zone in high-temperature formations.

Montarnal et al.[14] constructed an epoxy resin with reversible cross-linking structure based on a transesterification reaction and proposed the concept of a vitrimer for the first time. This kind of material has the strength characteristics of a thermosetting material under the condition of lower temperature. It has the self-healing characteristics of thermoplastic materials when encountering a high-temperature environment. This material can better solve the defects faced by conventional intelligent plugging materials in high-temperature fracture leakage formation, but its application in drilling or workover engineering has not been reported in the relevant literature. At present, the main component of the glass-like polymer is bisphenol A, which causes serious environmental pollution and is difficult to degrade. It requires special organic solvents to achieve chemical degradation. Therefore, a series of biobased vitrimer materials have been developed. According to the types of dynamic covalent bonds, biobased vitrimer mainly include three types: hydroxyl ester, Schiff base, and disulfide bond.[15,16] Altuna et al.[17] used soybean oil and citric acid to prepare a catalyst-free vitrimer. The material is based on the transesterification of β-hydroxyl and ester groups, and the relaxation time at 160 °C is about 2 h. Geng et al.[18] prepared a cross-linked Schiff vitrimer based on vanillin dialdehyde monomer by using an imine chemical method. It can be decomposed and recovered within 24 h in a 50 °C acidic solution. Cheng et al.[19] prepared a vitrimer with a double cross-linking network by using dicarboxylic acid and diamine monomer containing disulfide bonds and epoxidized natural rubber. The material has an excellent self-healing efficiency. After 60000 times of fixed strain stretching and 6 h of self-healing at 120 °C, the self-healing rate reaches 98%. The fatigue-damaged sample recovered its original strength. However, the biobased vitrimer mainly faces the disadvantages of poor temperature resistance, high cost of raw materials, and difficult degradation.

Aiming at the plugging problem faced by high-temperature fracture leakage and the defects of existing intelligent plugging materials, a kind of biobased epoxy resin was synthesized with vanillin and solidified with SA, and a kind of biobased temporary plugging material was developed by adding modified hydrophobic cellulose and catalyst. The high-temperature intelligent plugging mechanism of the new plugging material is revealed through thermal mechanical property tests, degradation performance analysis, and fracture pressure sealing tests.

2. MATERIALS AND METHODS

2.1. Materials. Vanillin, epichlorohydrin, tetrabutylammonium bromide, urea, sodium hydroxide, absorbent cotton, acetic anhydride, SA, and AZH were purchased from Shanghai Makclin Biochemical Co., Ltd. The traditional plugging material was obtained from Shijiazhuang Leite Mineral Products Co., Ltd. Gel material was purchased from Kaifeng Hengju Biotechnology Co., Ltd. Shape memory resin was obtained from Shanghai Yuyu New Material Technology Co., Ltd.

2.2. Sample Preparation. *2.2.1. Synthesis of Vanillin-Derived Epoxy.* Vanillin (10 g, 0.0657 mol, 1 equiv), epichlorohydrin (60.79 g, 0.657 mol, 10 equiv), and tetrabutylammonium bromide (2.12 g, 0.006576 mol, 0.1 equiv) were put into a round-bottom flask with a constant pressure funnel and a magnetic stirrer and kept at 117 °C for 2 h. The container was cooled to 60 °C, 30 wt % NaOH aqueous solution (10.51 g of sodium hydroxide, 24.52 g of water, 0.2628 mol of NaOH, 4 equiv) was dropped within 30 min, and the mixture was stirred for 3 h. The mixture was washed three times with 70 °C pure water, and the epichlorohydrin was removed by vacuum distillation (35 °C, 4 KPa; 70 °C, 20 KPa) (Figure 1).

2.2.2. Synthesis of Modified Hydrophobic Cellulose. Absorbent cotton was dissolved with alkaline solution and urea under 0 °C.[20] Then, stir vigorously for 2 min, precipitate cellulose with ethanol, wash and precipitate with excessive deionized water, and finally obtain cellulose solution after centrifugation and freeze-drying.

Cellulose was exchanged from aqueous solution to Ac_2O and heated at 110 °C for 1 h (Ac_2O with cellulose content of 0.02 g/mL); then catalyst was added (Ac_2O with I_2 content of 0.4 mg/mL) and the mixture was heated at 110 °C for 30 min.

https://doi.org/10.1021/acsomega.3c04663
ACS Omega 2023, 8, 36207−36217

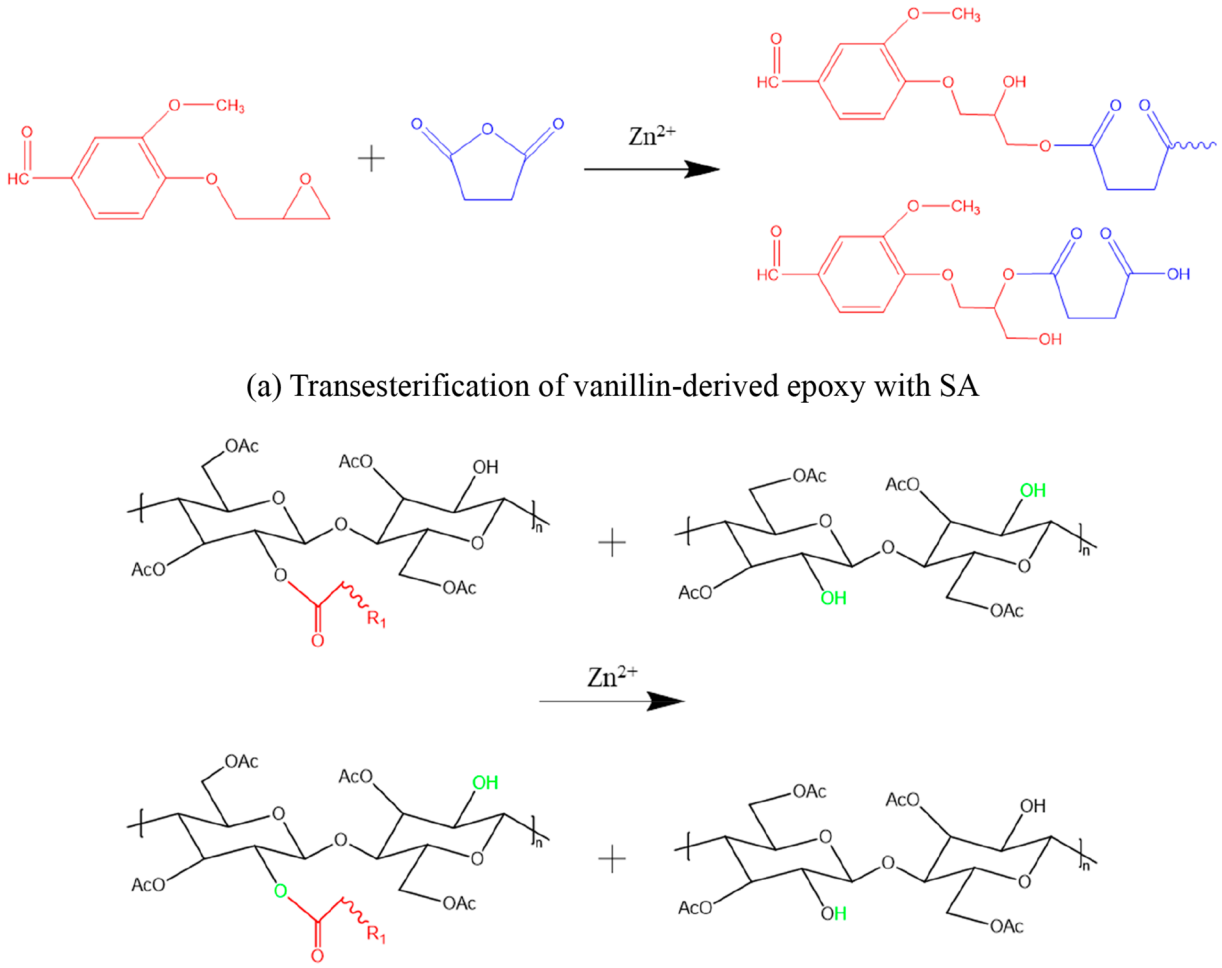

Figure 3. Synthesis route of biobased vitrimer with cellulose participation.

The modified cellulose sample was washed with acetone. The degree of substitution was 0.7 (Figure 2).

2.2.3. Synthesis of Biobased Vitrimer. The biomass glycidyl ether and SA were mixed with the same ratio of epoxy and anhydride. AZH was added as catalyst, and the unmodified cellulose, common cellulose, and modified hydrophobic cellulose were added, respectively. The solution was heated at 120 °C. The samples were poured into a polytetrafluoroethylene mold and cured at 120, 150, and 170 °C for 2 h, respectively. The three samples of the final product were pure biobased vitrimer, materials doped with 5% common cellulose, and materials doped with 5% modified hydrophobic cellulose. The synthesis route of biobased plugging material doped with cellulose is shown in Figure 3.

2.3. Characterization of Sample. *2.3.1. Infrared Spectrum Test.* A NICOLET iS50 FTIR spectrophotometer was used to test the Fourier transform infrared spectrum. Before the test, the sample was ground to 200 mesh and dried. 1 mg of the sample and 100 mg of potassium bromide were ground with a mortar and pressed into a transparent sheet.

2.3.2. Thermodynamic and Dynamic Mechanical Property Test. The change in mass with temperature was analyzed using SETLINE TGA. A 10 mg sample was heated in a nitrogen atmosphere.

The stress relaxation and T_g of the samples were measured by a dynamic thermal mechanical analyzer (DMA). The sample was tested with a tensile clamp, and the sample size was 30 × 5 × 3 mm^3. Stress relaxation was measured at 120 °C, and the influence of the heating time on mechanical properties of materials under constant temperature was analyzed. The test range was 30−150 °C to analyze the influence of temperature on the storage and loss moduli of materials.

2.3.3. Self-Healing Performance Test. A fixed size self-healing material plate was prepared by using a polytetrafluoroethylene mold, and fractures with a similar opening were scored by using a blade. The image recognition function of the optical microscope was used to measure the fracture opening. The sample to be tested was put into an oven to test the influence of the heating temperature and time on fracture opening. The calculation expression is shown as eq 1

$$\text{self healing ratio} = w_t/w_i \quad (1)$$

where w_i and w_t are the initial and any temperature moment of the fracture aperture, respectively.

https://doi.org/10.1021/acsomega.3c04663
ACS Omega 2023, 8, 36207−36217

2.3.4. Mechanical Property Test. Statistics show that the aperture of fracture leakage is generally 1−2 mm, so the particle size of the test plugging was 10−80 mesh (Lavrov, 2016).

Figure 4 shows that the press was tested by a manual hydraulic pump control. The mass of the test sample was 20 g.

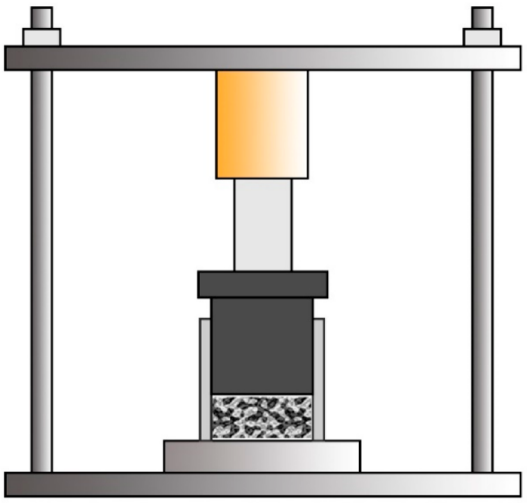

Figure 4. Schematic diagram of resilient performance test.

After it was loaded into the cylindrical mold, the mold was heated to the formation temperature with a heating sleeve. After the temperature was stabilized, the pressure was increased to 10 MPa, and the pressure was supplemented by the hydraulic pump to maintain a constant pressure for 5 min. The calculation equation of the resilient rate is shown in eq 2

$$\text{resiliency} = H_r/H_c - 1 \quad (2)$$

where H_c and H_r are the heights at the initial and compression stages, respectively.

Particle size variation was tested before and after extrusion to analyze the compressive strength, which is expressed in eq 3

$$\text{crushing rate} = m_p/m_{ip} \quad (3)$$

where m_{ip} and m_p are the masses at the initial and compression stages, respectively.

2.3.5. Degradation Performance Test. 40 g of the sample to be tested was added to 400 mL of 4% bentonite slurry, and NaOH of a certain concentration as added. The sample was hot rolled at 120 °C to test the influence of the alkaline environment and hot rolling time on the degradation degree of the material. The equation of decomposition rate is given as eq 4

$$\text{decomposition ratio} = m_r/m_{ir} \quad (4)$$

where m_r and m_{ir} are the masses at the residual and initial stages, respectively.

2.4. Comprehensive Performance Evaluation of Plugging Formula. *2.4.1. Rheology and Filtration Test.* 10% of the solution to be tested was added to 400 mL of 4% bentonite slurry, and the rheological property of the working fluid was tested with a KC-6ST rotary viscometer produced by KENMETER Shanghai Co., Ltd. The rheological and filtration performances of solution were calculated by an API testing method.

2.4.2. Fracture Plugging Performance Test. A dynamic plugging simulation experimental device with fixed fracture opening was used to test the plugging ability of the plugging formula.[21−24]

As indicated in Figure 5, the fracture dynamic plugging device uses nitrogen pressurization to simulate wellbore pressure. The disturbing effect of wellbore fluid circulation on the plugging layer was simulated using a conical stirring rod. The sample volume required for the plugging test was 1 L. The test temperature was 120 °C. Nitrogen iwass continuously pressurized at an interval of 0.5 MPa. After the plugging pressure was stable, no leakage occurred.

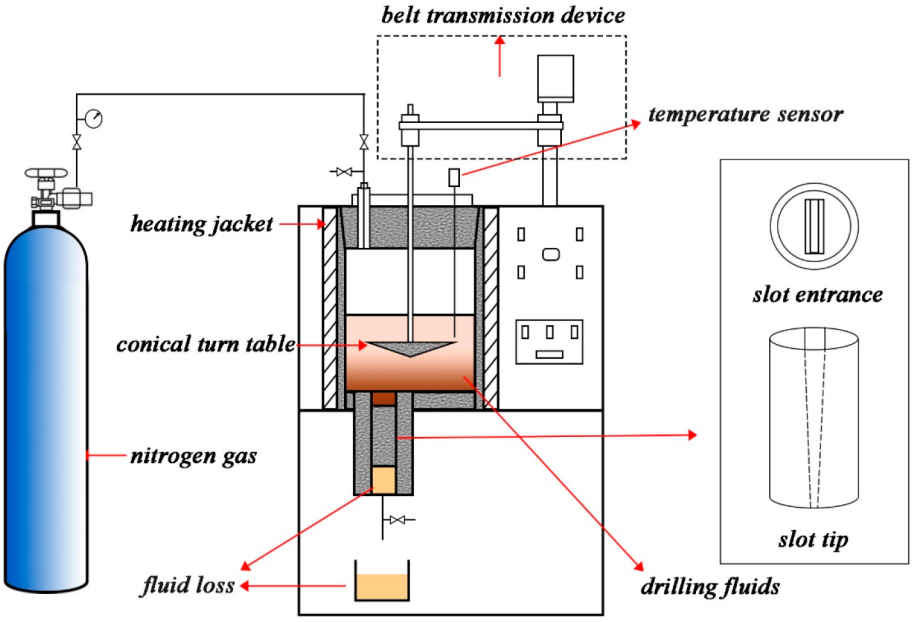

Figure 5. Dynamic plugging simulation experimental device.

https://doi.org/10.1021/acsomega.3c04663
ACS Omega 2023, 8, 36207−36217

3. RESULTS AND DISCUSSION

3.1. IR analysis. Figure 6 shows the infrared test results of vanillin, the synthetic intermediate vanillin-derived epoxy, and the final product vitrimer of plugging material.

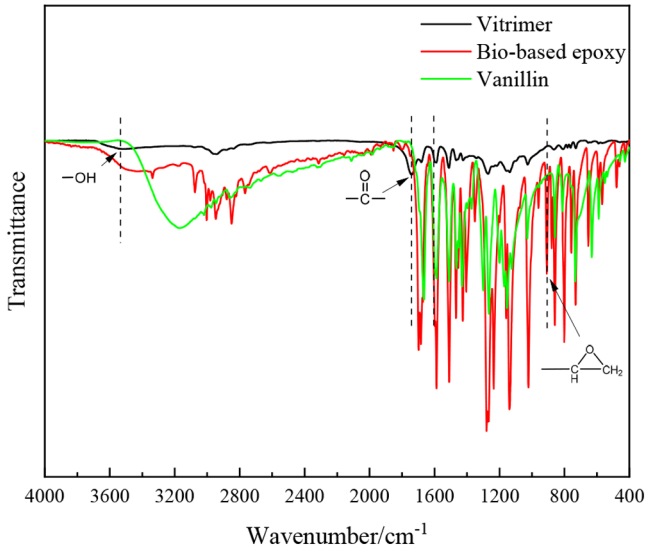

Figure 6. FTIR spectra.

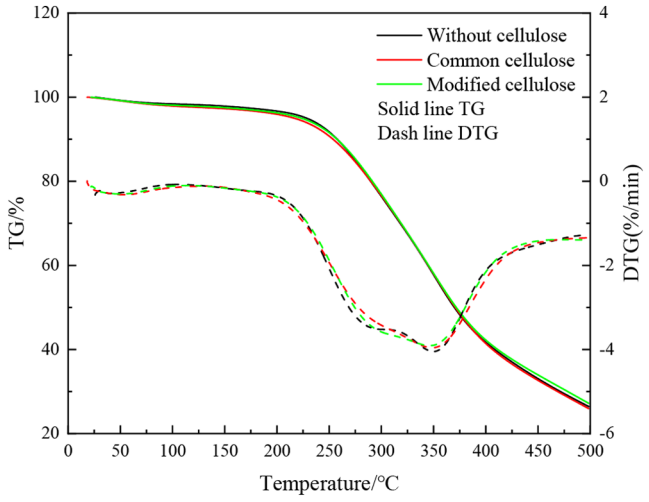

Figure 7. Thermogravimetric test results.

Figure 6 illustrates that the peak strength of vanillin-derived epoxy near 3100 cm^{-1} decreases due to the substitution reaction of phenol hydroxyl. Its infrared spectrum shows an epoxy group peak at 910 cm^{-1}, indicating that the epoxy group is grafted onto vanillin. In the final product of vitrimer, the epoxy group peak at 910 cm^{-1} almost disappeared, and carbon−oxygen double bond and hydroxyl group peaks were observed at 1750 and 3500 cm^{-1}, respectively. Due to the anhydride being opened by hydroxyl, the carboxyl group and epoxy group undergo an ester exchange reaction to form a dynamic ester bond.

3.2. Thermal Performance Analysis. Through the thermogravimetric performance test, the influence of doped modified cellulose and common cellulose on the temperature resistance of the material is compared and analyzed so as to determine the applicable formation temperature range.

As shown in Figure 7, the thermal decomposition rate is 10% at 20−255 °C, due to the evaporation of adsorbed water or combined water carried by the material. The decomposition rate reaches 50% at 255−410 °C, which is caused by macromolecular chain breaking at high temperature. The third stage is higher than 410 °C, and the mass loss tends to be gentle. Due to the carbonization process of the molecular chain, the mass loss rate decreases.

It can be seen from a horizontal comparison that the 5% mass loss temperature of materials with common cellulose is 217 °C, which is lower than that of materials without cellulose and doped modified cellulose. However, the addition and type of cellulose have little impact on the thermal stability of materials.

Figure 8 illustrates the dynamic thermomechanical properties. When the storage modulus is greater than the loss modulus, the material is more inclined to be an elastic solid, and when the two are equivalent, the material is a semisolid.

Figure 8a shows that the storage modulus increased significantly at high temperature when cellulose was contained, and the storage modulus of materials doped with modified cellulose was higher than that of materials doped with common cellulose. Because the modified cellulose has hydrophobic groups, it can be well dispersed in the synthetic product, which improves the structure density and makes the composite have better mechanical strength.

Figure 8b indicates that the T_g value increased by 7.1% and 8.6% when the plugging material contained common and modified cellulose, respectively. Due to the better dispersion performance, cellulose has a more significant effect on the increase of the cross-linking density, so it has a more obvious effect on the T_g.

3.3. Stress Relaxation and Self-Healing Performance Analysis. The stress relaxation effect under a 120 °C formation temperature was tested to analyze the dynamic thermal performance.

$1/e$ is the characteristic relaxation time. Figure 9 shows that the characteristic relaxation time is about 3500 s. The stress relaxation effect of the plugging materials without cellulose is obvious before 300 s, and the plugging materials with cellulose change significantly after 300 s. The addition of cellulose reduces the characteristic relaxation time of the plugging material significantly, indicating that the stress relaxation effect is more significant at this time. There are a large number of ester bonds or unsubstituted hydroxyl groups on the surface of cellulose, which can participate in the transesterification reaction under the action of high temperature and catalyst. Due to its highly hydrophobic properties, the modified cellulose can be highly dispersed in glass-+*l*ike polymer materials, providing a large number of active sites for the dynamic exchange of cross-linking networks. Therefore, the materials doped with modified cellulose have a better stress relaxation effect than those doped with common cellulose.

Self-healing characteristics of the fracture under a formation temperature of 120 °C were tested, and the influence of doped cellulose on its properties was discussed.

As indicated in Figure 10, the sealing material doped with modified cellulose has the most significant healing effect, which can reach 61% in 20 min, which is 69% higher than that of the traditional material. It reaches 42% in 20 min when containing common cellulose, which is 17% higher than that of plugging material doped with common cellulose. This result corresponds to the stress relaxation effect. Because the doping of

https://doi.org/10.1021/acsomega.3c04663
ACS Omega 2023, 8, 36207−36217

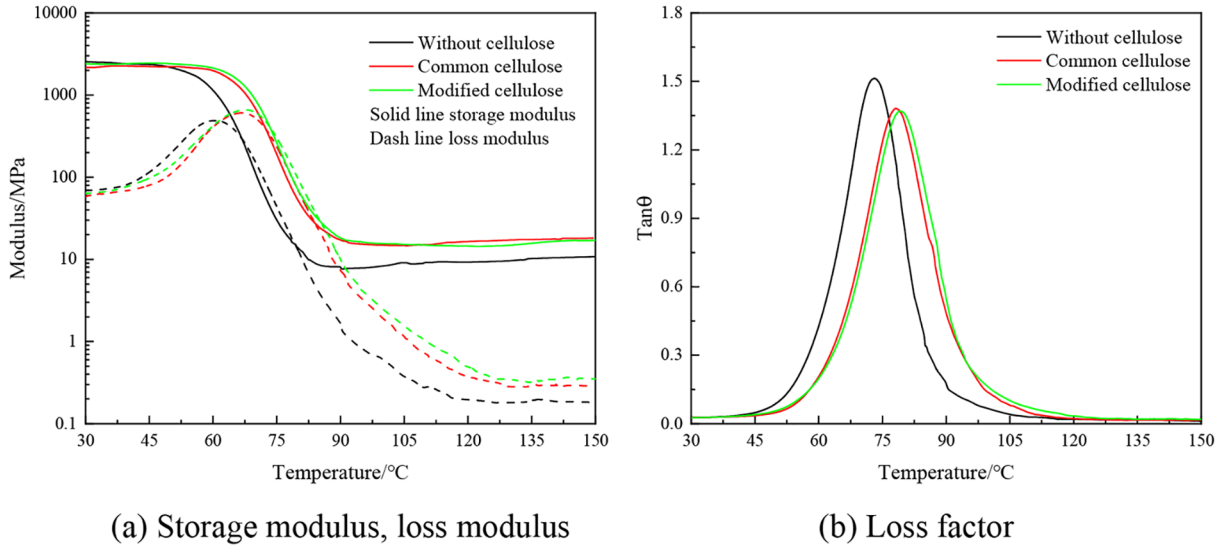

Figure 8. Results of dynamic thermomechanical properties of the plugging material.

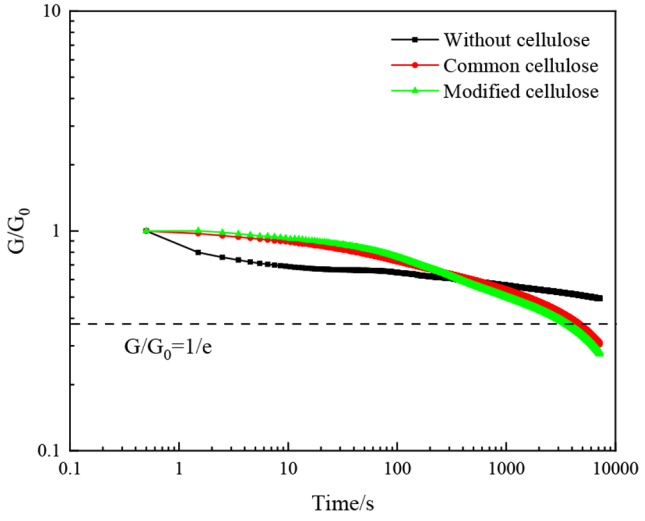

Figure 9. Stress relaxation characteristics of new biobased plugging materials.

cellulose provides ester bond or hydroxyl exchange sites for a dynamic transesterification reaction, under the condition of heat induction, a dynamic exchange reaction leads to faster reorganization of the cross-linking network structure, a shorter relaxation time of materials, and a remarkable self-healing effect.[25−28] Compared with traditional cellulose, modified cellulose provides a more active ester bond or hydroxyl site for a dynamic transesterification reaction due to its better hydrophobic dispersion performance.

3.4. Mechanical Property Analysis. In view of the leakage fracture opening range of a high-temperature gas well, the resilience and compression resistance of three kinds of particle size distribution plugging materials under formation temperature conditions are tested. The commonly used plugging materials such as calcium carbonate, elastic graphite, and nut shell are selected for comparative analysis. Figure 11 shows the test results of the resilience and compression resistance. Both represent the influence of fracture dynamic change caused by wellbore pressure fluctuation and fracture closure stress caused by in situ stress, respectively.

As shown in Figure 11, the resilience rate is more than 36% when the material contains modified cellulose, which is close to that of elastic graphite. The compression resistance of the new plugging material is better than that of traditional material, and the crushing rate is less than 17%. Since the new plugging material has a dynamic cross-linking network structure, a topology rearrangement can be realized. Therefore, it has good elastic deformation performance, can withstand large extrusion deformation, and can maintain the integrity of the structure under large deformation conditions.

A horizontal comparison shows that the plugging material has the best performance when it contains modified cellulose. This is because the homogeneous dispersion of hydrophobically modified cellulose and abundant ester bond or hydroxyl exchange sites provide favorable conditions for dynamic transesterification. In addition, cellulose improves the structure density, causing the plugging material to have better compressive strength.

3.5. Degradation Performance Analysis. In order to test the influence of an alkaline environment on the hydrolysis effect, plugging materials doped with modified cellulose were selected to test the influence of NaOH dosage on degradation performance at 120 °C. The degradation rates of different types of cellulose doped with 0.8% NaOH are compared and analyzed. The test results are shown in Figure 12.

As shown in Figure 12a, under the condition of hot rolling at 120 °C, there is almost no mass loss in the base mud. As the dynamic ester bonds break and hydrolyze to hydroxyl and carboxyl groups, the decomposition degree gradually accelerates with an increase of the alkalinity of the base slurry. Specifically, under the condition of 0.4% NaOH dosage, the decomposition rate increases to 80% at 5 h. Under the same degree of decomposition, the decomposition time is reduced to 2 h with 0.8% NaOH, which is shortened by 60%. When the NaOH content is 1.2%, the time required for 80% degradation degree is shortened to 0.5 h, and the degradation time is shortened by 90%.

As shown in Figure 12b, the degradability is obviously better when the material contains cellulose. Compared with the

https://doi.org/10.1021/acsomega.3c04663
ACS Omega 2023, 8, 36207−36217

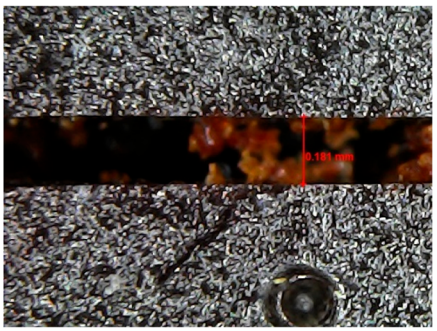

(a) Initial fracture width (without cellulose)

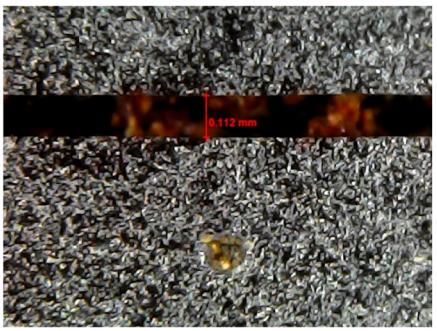

(b) Fracture width after 30 min (without cellulose)

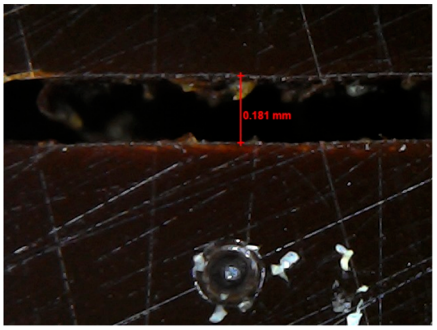

(c) Initial fracture width (common cellulose)

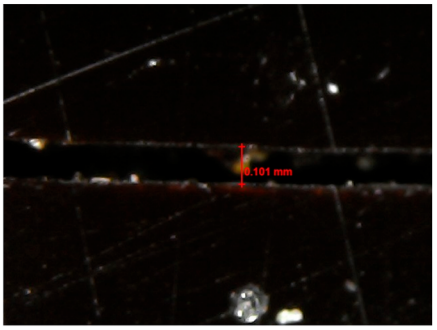

(d) Fracture width after 30 min (common cellulose)

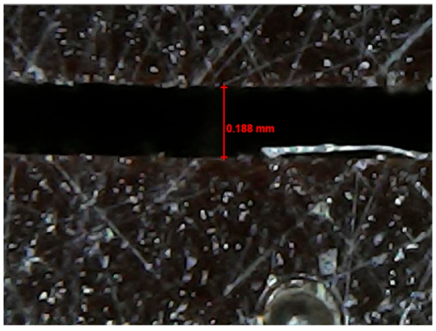

(e) Initial fracture width (modified cellulose)

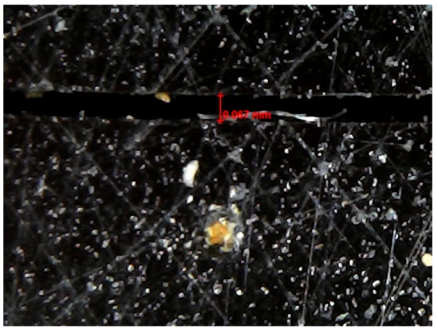

(f) Fracture width after 30 min (modified cellulose)

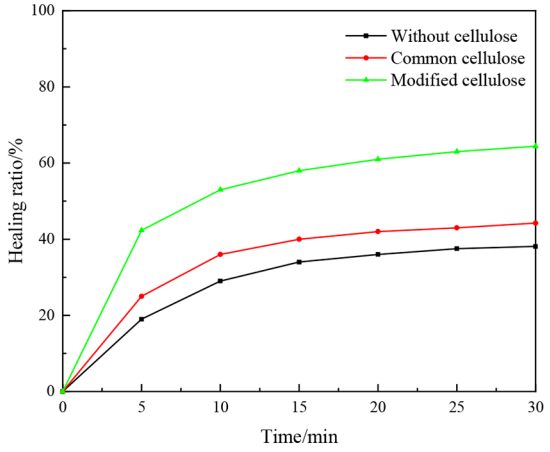

(g) Results of self-healing rate

Figure 10. Results of self-healing characteristics.

https://doi.org/10.1021/acsomega.3c04663
ACS Omega 2023, 8, 36207−36217

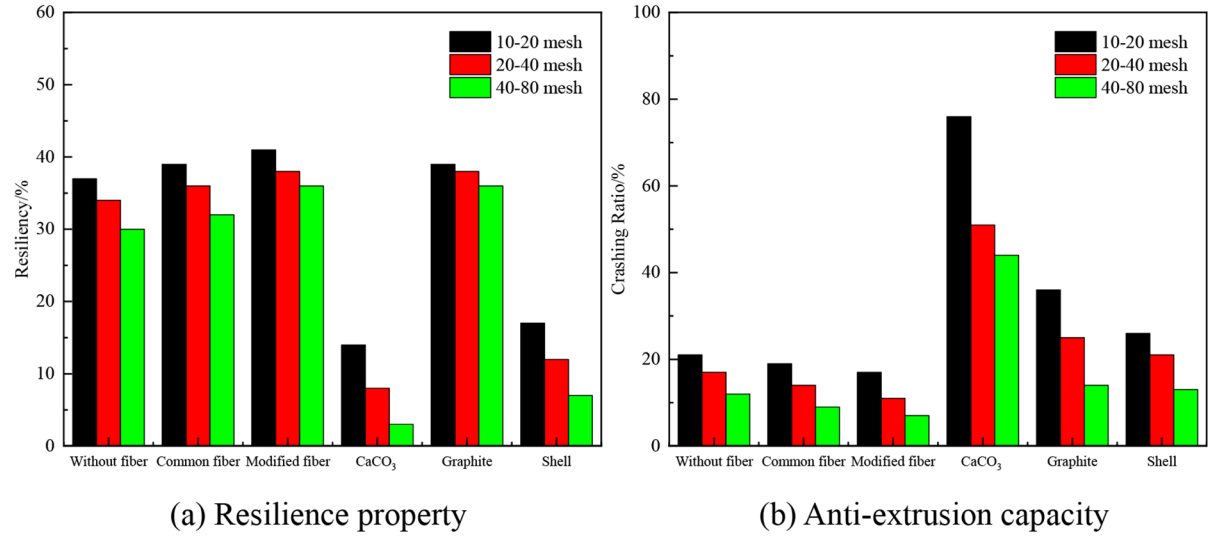

Figure 11. Results of mechanical property tests.

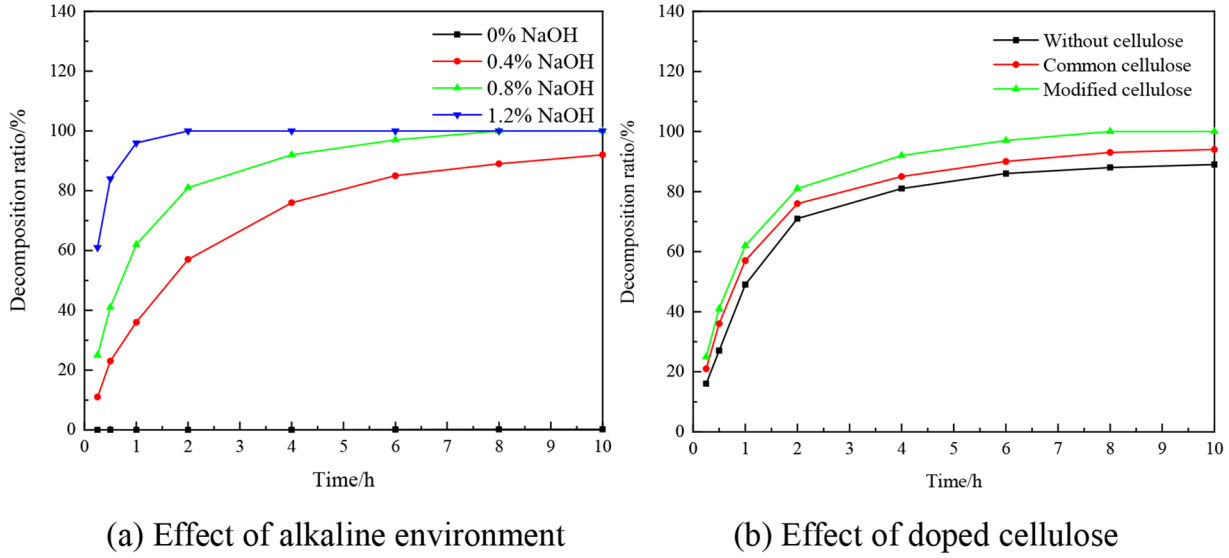

Figure 12. Comparison of residual solid contents after degradation.

Table 1. Influence of New Lost Circulation Material on Fluid Performance (120 °C/16 h)

sample	condition	AV (mPa s)	PV (mPa s)	YP (Pa)	gel (Pa/Pa)	FL_{API} (mL)
base slurry	before hot rolling	34	19	15	5/9	3.2
	after hot rolling	14	7	7	2/5	6.2
+ without cellulose	before hot rolling	35	22	13	3/7	3.4
	after hot rolling	15	10	5	1/5	4.0
+ common cellulose	before hot rolling	33	21	12	4/9	3.0
	after hot rolling	16	11	5	2/5	3.8
+ modified cellulose	before hot rolling	34	20	14	4/9	3.2
	after hot rolling	18	10	8	3/7	3.8

Table 2. Sealing Performance of Different Materials

fracture width (mm)	content (%)	pressure-bearing capacity (MPa)			
		gel	composite material	shape memory polymer	new material
2 × 1	5	8.0	10	10	10
3 × 2	8	6.5	7.5	9.5	10
4 × 3	10	4.5	5	8	10
5 × 4	15	2.5	4.5	6.5	10

degradation degree of 2 h, the degradation time of plugging materials doped with common cellulose is shortened by 7%, while that of plugging materials doped with modified cellulose is shortened by 14%. This illustrates that cellulose enhances the stress relaxation effect, and dynamic ester bonds are easier to degrade.

3.6. Rheology and Filtration Performance Analysis. The traditional chemical cementing materials are generally injected into the lost circulation zone in the form of slugs, which is easily caused due to the difficulty in effectively

https://doi.org/10.1021/acsomega.3c04663
ACS Omega 2023, 8, 36207−36217

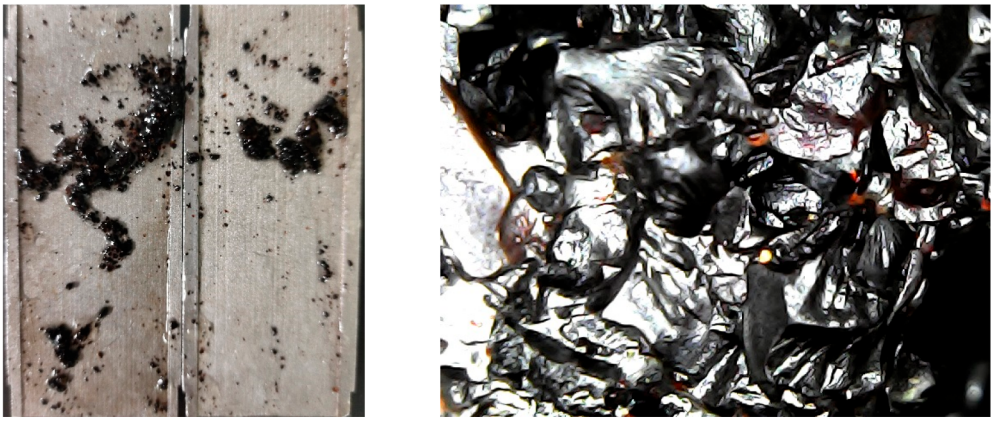

(a) Distribution of plugging particle (b) Micro morphology of plugging zone

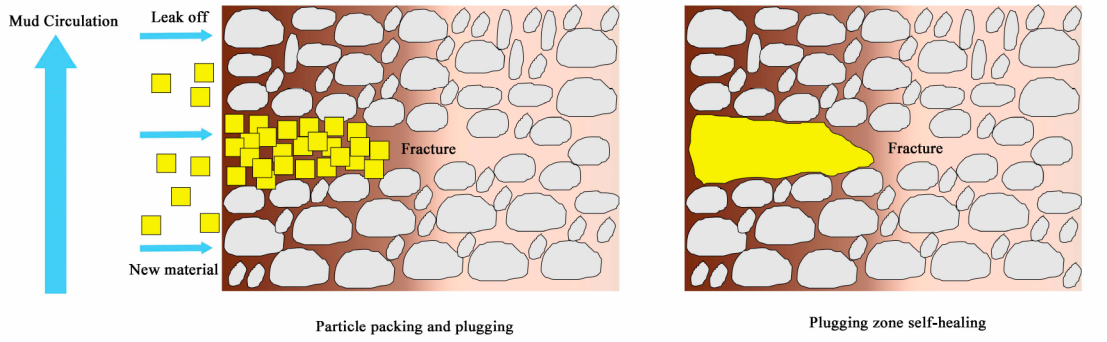

(c) Self-healing mechanism

Figure 13. Micro plugging mechanism.

controlling the cementing time. However, the new plugging materials can be injected in the form of particles while drilling or of slugs. The compatibility of the materials was analyzed by rheological and filtration tests. The particle size of plugging material was 40−80 mesh.

As shown in Table 1, the influence of new plugging materials on the rheology and filtration of base slurry is relatively small before hot rolling. After a 120 °C/16 h hot rolling treatment, the viscosity of the working fluid increased slightly and the filtration loss decreased significantly, indicating that the plugging properties were improved at high temperature. This shows that after it reaches the activation point of T_g, the material has viscoelastic characteristics and can block the micro pore channels through elastic deformation. Due to a significant stress relaxation effect and superior elastic deformation performance at high temperature, the material has the best plugging performance when it contains modified cellulose.

3.7. Analysis of Sealing Performance. The plugging performance under different fracture opening conditions is compared and analyzed by using a traditional particle composite plugging material, a chemical cementation gel material, and a temperature-sensitive smart shape memory polymer. Among them, the composition and proportion of composite plugging materials are calcium carbonate with shell, rubber, and fiber in the ratio 70:20:9.8:0.2. Composite plugging materials, shape memory polymers,and new plugging materials all adopt the rule to design particle size distribution and cooperate with base slurry to simulate plugging while drilling.[29−31] The gel material adopts the same quality, simulates slug construction, and is directly added to the simulationuipment. The components of the plugging experimental slurry are the polymer and bentonite.

As shown in Table 2, the shape memory polymer can self-adjust the structure through temperature-sensitive expansion. However, due to the influence of T_g, some particles expand rapidly before entering the fracture and lose the expansion filling effect.[32−35] Inert composites have excellent temperature resistance; however, their matching effect with fracture opening is subject to particle size optimization criteria, and the elastic deformation properties of some materials are relatively poor. The gel had good fluidity. After consolidation, the sealing zone has good compactness, but it faces the problem of insufficient temperature resistance. After long-term heating, the material is degraded at a high temperature, and the gel-forming time is difficult to control.

Figure 13 indicates that the plugging particle is mainly distributed near the fracture entrance according to D90 design criteria. Under the effect of high temperature, the granular materials self-heal to form a dense cementation structure. The

https://doi.org/10.1021/acsomega.3c04663
ACS Omega 2023, 8, 36207−36217

sealing zone formed after healing has a high hardness and does not flow out from the fracture outlet.

As indicated in Figure 13c, the new plugging material can be used with the plugging working fluid while drilling, and it can enter the leakage fracture channel under the effect of differential pressure. After the sealing zone is formed by accumulation, under the action of high temperature, the micropores formed by the accumulation of sealing particles are healed by a dynamic transesterification reaction, thus forming a dense sealing zone. In addition, the addition of hydrophobic modified cellulose gives the new material better mechanical strength.

4. CONCLUSIONS

The vanillin-derived epoxy was synthesized from vanillin, and modified hydrophobic cellulose was prepared by carboxymethyl acetylation. A new type of biobased, self-healing, degradable temporary plugging material with hydroxyl ester dynamic covalent bonds was synthesized.

The new plugging material shows good thermodynamic performance. The uniform dispersion of hydrophobic modified cellulose and abundant ester bonds or hydroxyl exchange sites accelerated the restructuring of the cross-linking network structure, which provided favorable conditions for improving the elastic deformation properties of materials. At the same time, the dynamic ester bond is easier to degrade under high-temperature and alkaline conditions.

The fracture sealing performance of the new material at a high temperature is excellent. Compared with traditional particle composite plugging materials, chemical cementation gel materials, and shape memory polymers, it has the best pressure bearing effect. Under the condition of 120 °C, the 5 × 4 mm fracture is plugged and the pressure is up to 10 MPa. Through the stress relaxation effect, the micro pores in the sealing zone can self-heal. Hydrophobically modified cellulose can be used to improve the cross-linking density of the material and enhance the compressive strength of the plugging zone.

AUTHOR INFORMATION

Corresponding Author

Jia Li − *Research Institute of Natural Gas Technology, PetroChina Southwest Oil & Gas Field Company, Chengdu, Sichuan 610213, People's Republic of China;* orcid.org/0000-0002-9549-6656; Email: li_jia01@petrochina.com.cn

Authors

Ming Wen − *PetroChina Southwest Oil & Gas Field Company, Chengdu, Sichuan 610051, People's Republic of China*

Shuang Liu − *Research Institute of Natural Gas Technology, PetroChina Southwest Oil & Gas Field Company, Chengdu, Sichuan 610213, People's Republic of China*

Qiang Liu − *PetroChina Southwest Oil & Gas Field Company, Chengdu, Sichuan 610051, People's Republic of China*

Complete contact information is available at: https://pubs.acs.org/10.1021/acsomega.3c04663

Notes

The authors declare no competing financial interest.

ACKNOWLEDGMENTS

This work was financially supported by the Research Project of Southwest Oil and Gas Field Company of PetroChina (20230303-18).

REFERENCES

(1) Lavrov, A. *Lost circulation: mechanisms and solutions*; Gulf Professional Publishing: 2016; pp 23−25.

(2) Mirabbasi, S. M.; Ameri, M. J.; Alsaba, M.; Karami, M.; Zargarbashi, A. The evolution of lost circulation prevention and mitigation based on wellbore strengthening theory: A review on experimental issues. *J. Pet. Sci. Eng.* **2022**, *211*, 110149.

(3) Pu, L.; Xu, P.; Xu, M.; Song, J.; He, M. Lost circulation materials for deep and ultra-deep wells: A review. *J. Pet. Sci. Eng.* **2022**, *214*, 110404.

(4) Bai, Y.; Zhang, Q.; Sun, J.; Lv, K.; Shang, X.; Liu, C.; Cheng, R.; Wang, F. Self-healing hydrogels and their action mechanism in oil-gas drilling and development engineering: A systematic review and prospect. *J. Nat. Gas Sci. Eng.* **2021**, *96*, 104250.

(5) Cui, K.; Jiang, G.; Xie, C.; Yang, L.; He, Y.; Shen, X.; Wang, X. A novel temperature-sensitive expandable lost circulation material based on shape memory epoxy foams to prevent losses in geothermal drilling. *Geothermics* **2021**, *95*, 102145.

(6) Magzoub, M.; Salehi, S.; Li, G.; Fan, J.; Teodoriu, C. Loss circulation prevention in geothermal drilling by shape memory polymer. *Geothermics* **2021**, *89*, 101943.

(7) Tabatabaei, M.; Taleghani, A. D.; Li, G.; Zhang, T. Shape memory polymers as lost circulation materials for sealing wide-opened natural fractures. *SPE Drill. Completion* **2021**, *36* (04), 931−942.

(8) Wang, Q.; Tian, L. F.; Song, P.; Liu, Z. Research on the Cement-Based Smart Lost-Circulation Control Material with Ti-Ni SMA. *In Advanced Materials Research* **2010**, *123*, 1015−1018.

(9) Tian, L. F.; Wang, Q.; Song, P.; Liu, Z. Research on the Cement-Based Smart Lost-Circulation Control Material with Cu-Zn-Al SMA. *In Advanced Materials Research* **2011**, *261*, 757−760.

(10) Mansour, A.; Ezeakacha, C.; Taleghani, A.; Salehi, S. Smart Lost Circulation Materials for Productive Zones. *SPE Annual Technical Conference and Exhibition*, San Antonio, Texas, USA, October 2017.

(11) Mansour, A.; Ahmed, K.; Taleghani; Arash, D.; Li, G. Smart Lost Circulation Materials for Wellbore Strengthening. *51st U.S. Rock Mechanics/Geomechanics Symposium*, San Francisco, California, USA, June 2017.

(12) Mansour, A. K.; Ahmed, K.; Dahi, T. Smart Loss Circulation Materials for Drilling Highly Fractured Zones. *SPE/IADC Middle East Drilling Technology Conference and Exhibition*, Abu Dhabi, UAE, January 2018.

(13) Gong, Z.; Zhang, G.; Zeng, X.; Li, J.; Li, G.; Huang, W.; Sun, R.; Wong, C. High-strength, tough, fatigue resistant, and self-healing hydrogel based on dual physically cross-linked network. *ACS Appl. Mater. Interfaces* **2016**, *8*, 24030−24037.

(14) Montarnal, D.; Capelot, M.; Tournilhac, F.; Leibler, L. Silica-like malleable materials from permanent organic networks. *Science* **2011**, *334*, 965−968.

(15) Chong, K. L.; Lai, J. C.; Rahman, R. A.; Adrus, N.; Al-Saffar, Z. H.; Hassan, A.; Lim, T. H.; Wahit, M. U. A review on recent approaches to sustainable bio-based epoxy vitrimer from epoxidized vegetable oils. *Ind. Crops Prod.* **2022**, *189*, 115857.

(16) Krishnakumar, B.; Pucci, A.; Wadgaonkar, P. P.; Kumar, I.; Binder, W. H.; Rana, S. Vitrimers based on bio-derived chemicals: Overview and future prospects. *Chem. Eng. J.* **2022**, *433*, 133261.

(17) Altuna, F. I.; Pettarin, V.; Williams, R. J. J. Self-healable polymer networks based on the cross-linking of epoxidised soybean oil by an aqueous citric acid solution. *Green Chem.* **2013**, *15*, 3360−3366.

(18) Geng, H.; Wang, Y.; Yu, Q.; Gu, S.; Zhou, Y.; Xu, W.; Zhang, X.; Ye, D. Vanillin-based polyschiff vitrimers: reprocessability and

https://doi.org/10.1021/acsomega.3c04663
ACS Omega 2023, 8, 36207−36217

chemical recyclability. *ACS Sustainable Chem. Eng.* **2018**, *6*, 15463−15470.
(19) Cheng, B.; Lu, X.; Zhou, J.; Qin, R.; Yang, Y. Dual cross-linked self-healing and recyclable epoxidized natural rubber based on multiple reversible effects. *ACS Sustainable Chem. Eng.* **2019**, *7*, 4443−4455.
(20) Xiong, X.; Duan, J. Dissolution and Application of Cellulose in NaOH/Urea Aqueous Solution. *Role of Green Chemistry in Biomass Processing and Conversion* **2012**, 205−240.
(21) Mirabbasi, S. M.; Ameri, M. J.; Alsaba, M.; Karami, M.; Zargarbashi, A. The evolution of lost circulation prevention and mitigation based on wellbore strengthening theory: A review on experimental issues. *J. Pet. Sci. Eng.* **2022**, *211*, 110149.
(22) Xu, C.; Kang, Y.; You, L.; You, Z. Lost-circulation control for formation-damage prevention in naturally fractured reservoir: mathematical model and experimental study. *SPE J.* **2017**, *22*, 1654−1670.
(23) Yan, X.; Xu, C.; Kang, Y.; Shang, X.; You, L.; Jing, H. Mesoscopic structure characterization of plugging zone for lost circulation control in fractured reservoirs based on photoelastic experiment. *J. Nat. Gas Sci. Eng.* **2020**, *79*, 103339.
(24) Bai, Y.; Dai, L.; Sun, J.; Lv, K.; Zhang, Q.; Shang, X.; Liu, C.; et al. Experimental study on an oil-absorbing resin used for lost circulation control during drilling. *J. Pet. Sci. Eng.* **2022**, *214*, 110557.
(25) Zhao, Z.; Sun, J.; Liu, F.; Bai, Y.; Wang, R. A laboratory study of self-healing hydrophobic association gels used as lost circulation material. *Colloid Surface A* **2022**, *646*, 128964.
(26) Yang, L.; Xie, C.; Ao, T.; Cui, K.; Jiang, G.; Bai, B.; Tian, W.; et al. Comprehensive evaluation of self-healing polyampholyte gel particles for the severe leakoff control of drilling fluids. *J. Pet. Sci. Eng.* **2022**, *212*, 110249.
(27) Li, J.; Xiong, Y.; Zhang, Y.; Lan, K. A novel self-healing and degradable plugging material for high temperature gas well. *J. Mol. Liq.* **2023**, *376*, 121473.
(28) Yang, L.; Li, Y.; Gou, Y.; Wang, X.; Zhao, X.; Tao, L. Improving tumor chemotherapy effect using an injectable self-healing hydrogel as drug carrier. *Polym. Chem.* **2017**, *8*, 5071−5076.
(29) Hands, N.; Kowbel, K.; Maikranz, S.; Nouris, R. Drill-in fluid reduces formation damage, increases production rates. *Oil Gas J.* **1998**, *96* (28), 65−69.
(30) Zhao, X.; Qiu, Z.; Gao, J.; Ren, X.; Huang, W.; et al. Mechanism and effect of nanoparticles on controlling fines migration in unconsolidated sandstone formations. *SPE J.* **2021**, *26* (06), 3819−3831.
(31) Zhao, X.; Qiu, Z.; Sun, B.; Liu, S.; Xing, X.; Wang, M. Formation damage mechanisms associated with drilling and completion fluids for deepwater reservoirs. *J. Pet. Sci. Eng.* **2019**, *173*, 112−121.
(32) Lashkari, R.; Tabatabaei-Nezhad, S. A.; Husein, M. M. Shape Memory Polyurethane as a Drilling Fluid Lost Circulation Material. *Macromol. Mater. Eng.* **2021**, *306*, 2100354.
(33) Lashkari, R.; Tabatabaei-Nezhad, S. A.; Husein, M. M. Evaluation of shape memory polyurethane as a drilling fluid lost circulation and fracture plugging material. *Geoenergy Sci. Eng.* **2023**, *222*, 211445.
(34) Jinsheng, S. U. N.; Yingrui, B. A. I.; Cheng, R.; Kaihe, L. Y. U.; Fan, L. I. U.; Jie, F. E. N. G.; Hao, H. A.; et al. Research progress and prospect of plugging technologies for fractured formation with severe lost circulation. *Pet. Explor. Dev.* **2021**, *48*, 732−743.
(35) Wang, C.; Sun, J.; Long, Y.; Wang, R.; Qu, Y.; Peng, L.; Gao, S.; et al. A re-crosslinkable composite gel based on Curdlan for lost circulation control. *J. Mol. Liq.* **2023**, *371*, 121010.

https://doi.org/10.1021/acsomega.3c04663
ACS Omega 2023, 8, 36207−36217